

Effect Of Speed And Contact Pressure On The Wear Rate Of Automotive Brake Pad.

¹O. C. Nwufo,²K. M. D. Ezeji, ³C. F. Nwaiwu and ⁴C. A. Okoronkwo

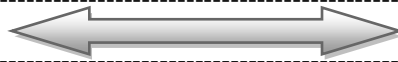
¹Department of Mechanical Engineering, Federal University of Technology, Owerri, Imo State, NIGERIA.

-----ABSTRACT-----

An Experimental Brake Pad Test Rig was designed and constructed using readily available materials. The equipment was designed to test automobile disc brake pad wear and effectiveness at various speeds and braking forces. To determine its functionality a wear test was conducted on a commercial brake pad at various speeds and brake forces. This prototype test rig can be used in testing the brake pad of different vehicle such as Toyota, Mitsubishi, Volvo, Peugeot, and other brands of interest. With little modification, this product can be commercialized.

Keywords: Automobile, Brake Pad, Wear, Test Rig.

Date of Submission: 28 Feb2013



Date Of Publication: 20, April.2013

NOMENCLATURE

a_f – Application factor
 A – Area
 C – Centre Distance
 C_{10} – Catalog Rating
 D – Diameter
 E – Elastic Modulus of the Material
 f – Pad Friction Coefficient
 F_c – Critical Force
 F_a – Axial Load
 F_D – Desired Load
 F_r – Radial Load
 g – Acceleration Due to Gravity
 I – Moment of Inertia
 K_m – Combined shock and fatigue factor applied to bending moment
 K_t – Combined shock and fatigue factor applied to torsion moment
 L – Length between supports
 L_c – Length of column
 L_D – Desired life
 L_p – Length of belt
 L_r – Rated life
 M – Maximum Bending Moment
 N – Rotational speed
 P – Power
 P_{av} – Average Pressure of the Pad
 R – Radius of Pad
 R_D – Reliability Factor
 T – Torsional Moment
 T_e – Equivalent Twisting Moment
 T_f – Frictional Torque
 V – Rotating Factor
 W_i – Weight of the i th location
 X – Distance from Neutral Axis
 y_i – Deflection of the i th body location
 Z – Section Modulus
 ζ_s – Allowable combined shear stress for bending and torsion

ω – Angular Velocity

ω_s – Critical speed

σ_b – Bending Stress

δ – Static Deflection

I. INTRODUCTION

Over the years, vehicles have become progressively faster and one of the most important considerations in the running and control of these modern cars is the braking system, which must be capable of decelerating the vehicle at a faster rate than the engine is able to accelerate it. According to Oguzie G.C.N. (2001), a car with good brakes should come to rest within 30m driving at 45km/hr. One of the most manifested causes of failure of the brake system of an automotive is the use of substandard brake pads. The presence of different types of brake pads in the Nigerian market today makes it imperative for one to make clear distinctions with regards to quality and performance. The important physical properties of interest to the vehicle users include the wear rate and effectiveness of the brake pads. Borjesson, N., et al (1993) noted that, other consumer demands include durability, safety and low cost which are functions of the above mentioned physical properties. In order to be able to select the right products, wear and effectiveness tests could be conducted on the various locally available brake pads in the Nigerian market. During the early part of the development of friction materials, several types of testing machines were developed, which were aimed at making brake systems safe, predictable in performance and reliable in service (Smiles, 1995). Some of these machines include a variety of laboratory-scale testing machines ranging from massive inertial dynamometer with electronic controls and sensors to small rub-shoe machines that can sit on a bench top. Others are Gould recording instruments, Euro type test equipment, FAST (Friction Assessment and Screening Test) machine, Chase machine, etc (Blau, 2001).

However the above types of equipment are very costly and scarce in developing countries such as ours, hence the need to develop an affordable test machine with high local content arises. This work focuses on the development of experimental brake pad test rig equipment as a means of determining the performance and quality of an automotive brake pad by simulating the braking system and conditions of a vehicle on which the pads are to be used. The major aim of this project is to develop an experimental brake pad test rig. This equipment will then be used to:

- Investigate the effect of speed and contact pressure on the wear rate of locally available automotive brake pad materials.
- Investigate the average stopping time and hence the effectiveness of the brake pad materials at different speeds.

The results obtained will be used to compare the wear rates and effectiveness of readily available automotive brake pads.

1.1. LIMITATION OF THE TEST RIG

Blau, P.J (2001) noted that the brake performance is affected not only by its materials and vehicle hardware design but also significantly by:

- The driver's behavior and vehicle usage;
- The state of adjustment of the brake hardware;
- The overall environment in which the vehicle is driven;
- Possible influences of braking control systems; and
- Aerodynamics in the wheels.

Thus no workshop test can perfectly simulate driving conditions, not even the test rig.

II. DESIGN METHODOLOGY

2.1. DESIGN DESCRIPTION

The schematic representation of the flywheel type test rig is as shown in figure 2. It consists of a brake disc and caliper assembly, brake booster and master cylinder unit, electric motor, main driveshaft, flywheel weights and mechanical actuator. The brake disc is mounted on a shaft driven via an electric motor as the prime mover, while the caliper, the mechanical actuator and some other components are bolted to the frame of the rig. The flywheel attached to the shaft enables the inertia of a vehicle to be simulated and thus boosts the shaft's inertia when it is driven by the motor. The rig also incorporates a hydraulic circuit fitted with a pressure gauge to measure the pressure in the fluid line from which the force with which the brake pads push against the disc can be estimated. The hydraulic line also has a boosting device (servo unit). The rig also has a limit switch attached to the frame near the brake pedal such that it turns off the electric motor when the pedal is depressed. The frame

is made from square channels and angle iron. The brake disc, pads, and caliper of a Volvo 240 model vehicle were used and the vacuum for servo assistance was achieved by the use of a small vacuum pump.

2.2. MODE OF OPERATION

First a set of brake pads to be tested is coupled into the caliper of the brake assembly. The shaft is then set in motion by the electric motor. The disc and flywheel both rotate until a stable speed is achieved. When the speed stabilizes, the brake circuit is actuated mechanically by depressing the brake pedal with the foot. As this is done, the limit switch turns off the motor and the shaft rotates by virtue of its inertia until it is brought to rest via the action of the pads against the disc. The time taken for the shaft to come to rest is measured and recorded. After the test, the brake pads are brought out for visual inspection and measurements for wear in terms of reduction in thickness. The test is carried out at different speeds defined by the ratios of the pulley diameters in the belt drive.

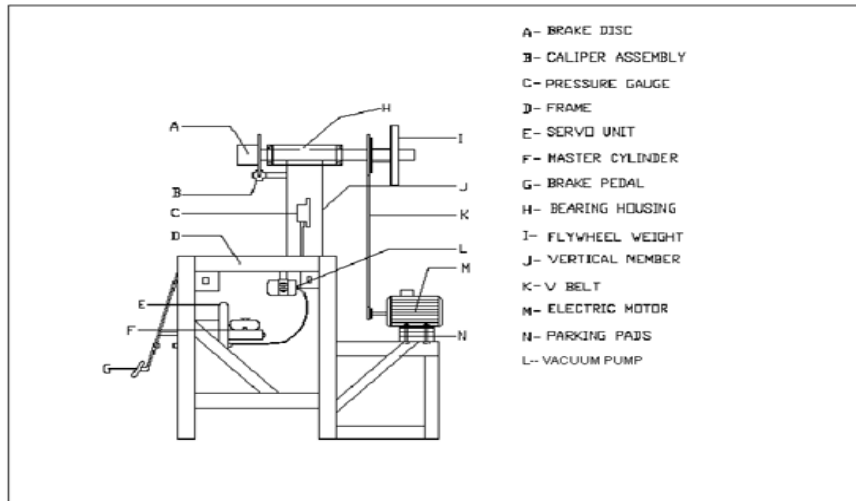


Fig 1 Test Rig Assembly

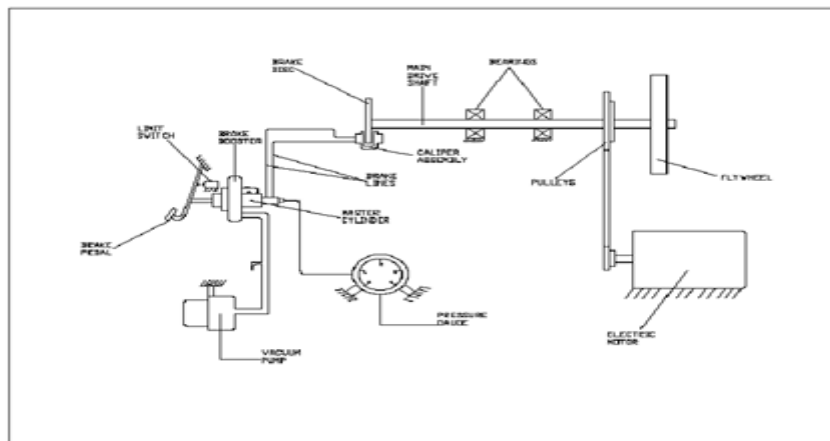


Fig 2 schematic representation of the test rig

2.3. DESIGN OF RIG ELEMENTS

2.4 SELECTION OF ELECTRIC MOTOR

A 2-horsepower (1.5KW) was found to be suitable in supplying the rotational energy needed to turn the flywheel weights and brake disc.

2.5 MAIN DRIVESHAFT

Using ASME code for shaft design (Khurmi and Gupta; 2005);

$$D^3 = \frac{16}{\pi \tau_s} \sqrt{(MK_m)^2 + (TK_t)^2} \dots (1)$$

$$T_e = \sqrt{(MK_m)^2 + (TK_t)^2} \dots (2)$$

Where:

T_e = Equivalent twisting and bending moment (Nm).

D = Shaft diameter (m).

ζ_s = Allowable combine shear stress for bending and torsion (N/m²).

K_m = Combined shock and fatigue factor applied to bending moment.

K_t = Combined shock and fatigue factor applied to torsional moment.

M = Maximum bending moment (Nm).

T = Torsional moment (Nm).

2.6 DETERMINATION OF TORSIONAL MOMENT (T)

Power transmitted

$$P = \omega T = \frac{2\pi NT}{60} \dots(3)$$

Where:

ω = Angular velocity (radians per seconds).

N = Revolutions per minute (rpm).

2.7 WHIRLING OF SHAFT

When shafts are subjected to concentrated loads, the shaft tends to deflect. Hence there is need to determine the critical speed of the main driveshaft above which resonance occurs so that the test rig could be operated safely. This critical speed is determined using the following equation (Shigley and Mischke; 2004) for shafts with uniform diameter, and simply supported, with point loads. For an ensemble of attachments, Rayleigh's method for lumped masses gives;

$$\omega_s = \sqrt{\frac{g \sum W_i y_i}{\sum W_i y_i^2} \dots} (4)$$

Where

ω_s = critical speed of the shaft, (rads/sec), g = acceleration due to gravity, (N/m²), W_i = weight of the i th location, (N) and y_i = deflection of the i th body location, (m).

Also the influence coefficients are given by;

$$\delta_{ij} = \frac{b_j x_i}{6E_s I L} (L^2 - b_j^2 - x_i^2) \quad x_i \leq a_i$$

$$= a_j \frac{(L-x_i)(2Lx_i - a_j^2 - x_i^2)}{6E_s I L} x_i > a_i \dots(5)$$

Where

L = length between supports (m), E_s = Elastic modulus for steel = 270Gpa, $I = \frac{\pi D^4}{64}$ = circular moment of inertia (m⁴) and D = diameter of shaft (m).

Note: Equation (5) above is valid for either two point load placed between the supports or on one side of the supports.

$$\sum W_i y_i = W_1 y_1 + W_2 y_2 \dots (6)$$

$$\sum W_i y_i^2 = W_1 y_1^2 + W_2 y_2^2 \dots (7)$$

$$y_1 = \left| W_1 \delta_{11} + W_2 \delta_{12} \right| \dots (8)$$

$$y_2 = \left| W_1 \delta_{21} + W_2 \delta_{22} \right| \dots (9)$$

2.8 FRAME DESIGN

CRITICAL BUCKLING LOAD

It is known that when columns are subjected to compressive loads, they tend to fail by buckling when their critical load is attained. For a square channel iron column fixed at one end and free at the other end, the Euler's formula (equation 14) is used to determine the critical buckling load of the rig frame.

$$P_{critical} = \pi^2 E_i I_R / 4 L_c^2 \dots (10)$$

Where, L_c = length of the column = 0.6m, E_i = Elastic modulus for iron = 100GPa and $I_R = bh^3/12$ = lower rectangular moment of inertia for the section, (m^4)

2.9 BENDING STRESS

The horizontal members of the frame which support the electric motor and other components are subjected to bending moments and shearing loads. The bending stresses are calculated using equation 11 below

$$\sigma_b = MX/I_R = M/Z \dots (11)$$

(Shigley and Mischke; 2004)

Where, σ_b = bending stress, (N/m^2), M = maximum bending moment (Nm), I_R = rectangular moment of inertia, (m^4), X = distance from neutral axis of the cross section and $Z = bh^2/6$ = sectional modulus, (m^3).

Hence for this design, a 50 x 50 x 5mm square channel and angle iron were found to be suitable in carrying the components of the test rig.

2.10 DETERMINATION OF FRICTIONAL TORQUE ON THE BRAKE DISC

Using Pascal's law for critical force on the pad, $F_c = PA$

This implies that $F_c = \pi R^2 P_{av} \dots 12$

Where, R = radius of the pad (50mm) and P_{av} = average pressure on the pad

The retarding or frictional torque (T_f) on the brake disc can be obtained from equation 17 below;

$$T_f = f F_c r_e * \text{number of pads} \dots (13)$$

Where, f = pad friction coefficient (0.35), F_c = critical force (7853.98N), r_e = effective radius = $r_d - R/2$ (0.105m), r_d = rotating radius of the disc (0.13m)

2.11 DETERMINATION OF SUITABLE PRESSURE GAUGE FOR THE RIG

To measure the pressure in the brake lines, it is important to select a suitable pressure gauge. According to Mudd (1986), the maximum force needed at the pedal to fully operate the brakes should not exceed 180N. Therefore applying Pascal's law ($P=F/A$), a pressure gauge ranging from 0 to 14bar was found suitable.

2.12 SELECTION OF FLYWHEEL WEIGHT

For the test rig, a flywheel is necessary in order to boost the shaft's inertia when it is driven by the electric motor. The mass moment of inertia of the flywheel is used to simulate the inertia of the vehicle. For the laboratory type test rig, an 8kg (78.48N) weight was found suitable as a flywheel.

2.13 SELECTION OF PULLEYS AND BELTS

Pulley diameters and belt length were selected to serve within the operating parameters of the rig. Hence pulley diameters were selected as $\varnothing 110$ mm on the drive shaft sheave and $\varnothing 68$ mm on the electric motor. The length of V-belt to be used can be calculated from the equation below (Khurmi and Gupta; 2005)

$$L_p = 2C + \pi/2(D_b + d_s) + (D_b - d_s)^2/4C \dots 14$$

Where

L_p = length of the belt, (m), C = center to center distance, (m), D_b = diameter of the big sheave, (m) and d_s = diameter of small sheave, (m).

The cross sectional dimensions of the V-belts have been standardized by manufacturers, with each section designated by an alphabet for sizes in inch dimensions. Metric sizes are designated in numbers. Dimensions, minimum sheave diameters and the horsepower range for each of the lettered sections are listed in ASME (American society of mechanical engineers) standard V-belts table (Shigley et al; 2004).

Suitable V-belts were selected from the ASME table for V-belts drive based on the horsepower rating, minimum sheave diameters, and the center distance. From the ASME table, A51 V-belt section with thickness $b=12.5$ mm were selected for the various speeds.

2.14 BEARING SELECTION

Single row deep groove ball bearings will take radial loads as well as some thrust load. Roller bearings will carry greater radial load than ball bearing of the same size because of greater contact area (Shigley et al; 2004).

Bearing load life at rated reliability of 90% has a reliability factor of 0.96 (Khurmi and Gupta, 2005; Shigley et al, 2004). The catalog rating of a particular bearing can be calculated from the equation below;

$$C_{10} (L_R N_r 60)^{1/a} = a_f F_D (L_D N_D 60)^{1/a}$$

This implies that

$$C_{10} = a_f F_D (L_D N_D 60 / 10^6)^{1/a} \dots (15)$$

Where, N_r =rated speed (rpm), L_r =rated life (hrs), N_D =desired speed (rpm), L_D =desired life (hrs), F_D =desired load (KN), C_{10} =catalog rating (KN), a_f =application factor = 1.2 and $a=3$ for ball bearing and $10/3$ for roller bearings

Equation 15 can be rewritten as

$$G_O = a_f F_D [X_D / (X_O + (\theta - X_O) (1 - R_D) 1/b)] 1/a \dots (16)$$

Where, $X_D = L/L_{10} = 60 L_D N_D / 10^6$, $X_O = 0.02$, $\theta = 4.46$, $b = 1.483$; and R_D = reliability factor at 90% reliability = 0.96

2.15 DETERMINATION OF DESIRED LOAD (EQUIVALENT LOAD) F_e

Ball Bearing

The equivalent load F_e for ball bearings for combined radial and thrust loading can be obtained from the equation below

$$F_e = V f_{r1} x + y f_a \dots (17)$$

Where, V = rotating factor ($V=1$ for inner ring rotation and 1.2 for outer ring rotation), x = the ordinate intercept, y = slope of the line for $f_a / V f_r > e$, f_r = radial load, (N) and f_a = axial load, (N).

Both x and y can be read directly from ABMA (American bearing manufacturers association) table of equivalent radial load factors for ball bearings considering the value of the factor f_a / C_0 . (where C_0 is the static load rating of the bearing).

Considering the bearing reactions as shown in the free body diagram of the shaft, $f_a = 578.57N$ and $f_r = 578.57N$. Reading directly from tables for $(f_a / V f_r) > e$, $x = x_2 = 0.56$ and $y = y_2 = 1.99$. Applying equation 20, F_e equals $1475.35N$.

Roller Bearing

The equivalent load of a roller bearing can be determined from either of the two equations whichever gives a greater value.

$$P_A = 0.4 f_{r1} + K_1 F_{Aa} \dots (18)$$

$$P_B = f_{r2}$$

$$F_{Aa} = \frac{0.47 f_{r2}}{K_1} (K_1 = 1.67) \dots (19)$$

For the test rig, one 02-35mm series single row deep groove ball bearing and one 02-35mm cylindrical roller bearing were selected to take up the entire radial load as well as thrust load.

2.15 RIG CONSTRUCTION DETAILS

FRAME CONSTRUCTION

The test rig frame was constructed with $50mm \times 50mm \times 5mm$ square channel, $50mm \times 50mm \times 4mm$ angle iron. For greater strength and rigidity, all the members were welded together using MS G12 electrode.

III. MAIN DRIVE SHAFT

The bearing housing was made with a 250mm×210mm×6mm thick plate which was folded to 210mm×Ø80mm cylindrical shape to accommodate the two bearings with external diameters of 72mm. The main drive shaft was machined down on the center lathe from Ø55mm to Ø35mm. One end of the shaft has a rear wheel axle head to accommodate the disc brake. The main drive shaft passes through the centralized bearing holes. Suitable sheaves to accommodate the V-belts and the flywheel weight were obtained from the market, after which holes of Ø40mm were bored on the main shaft sheave as well as the flywheel to accommodate a bushing, while a hole of Ø20mm was bored on the electric motor sheave. The drive shaft sheave and the flywheel were welded to a common bushing which was then force fitted into the main shaft and finally secured with a set screw. The bearing housing, shaft, disc, sheave and the flywheel were mounted on top of the 100mm×100mm×8mm square channel frame.

3.1 OTHER RIG COMPONENTS

The electric motor, the limit switch and other switches, the pressure gauge, and the vacuum pump were bolted to the angle iron and square channel frame respectively. The brake pedal, servo and master cylinder unit were bolted to the frame for rigidity and maintainability. The hub/caliper unit was bolted on a set screw which was welded to the vertical member of the frame. Subsequently, the brake was properly connected with flexible metallic brake pipes and rubber hoses. Finally all the welded joints were filed and the entire rig elements were sanded and properly painted.

3.2 MAINTAINABILITY OF THE RIG

During the design of the test rig, the aspect of maintainability for the rig was seriously taken into consideration in the following ways;

- a. Bolts and nuts were used to secure the various components onto the frame, in place of welds. This was done to ensure easy dismantling of the components for maintenance services;
- b. The components were positioned in such a way that each could be dismantled separately.

IV. PERFORMANCE TESTS AND RESULTS

A performance test was carried out on the constructed rig to determine its functionality by investigating the effect of speed and contact pressure on wear of a brake pad material. The test was carried out on two sets of brake pads from different manufacturers which for simplicity are labeled pads A and B respectively. The test was carried out in two phases viz: Keeping contact pressure constant and varying rotating speed of the brake disc (ranging from 695 to 1248 rpm) Keeping rotating speed constant and varying contact pressure (ranging from 8 to 14bar)

4.1 RESULTS

The wear rates and average stopping times of both sets of brake pads being tested under the above conditions were measured and recorded as shown in the following tables. Table 1 presents data on the effect of speed on wear in terms of reduction in thickness for the two sets of brake pads. From the table, it can be deduced that the average wear rate of pad A at a constant pressure of 10 bar was 6.115×10^{-3} mm per brake application and that of pad B was 7.205×10^{-3} mm per brake application, which are slightly higher than the average wear rate of a typical automotive brake pad material, that is, 5×10^{-4} mm per brake application as reported by Blau, (2001). Table 2 presents data on the effect of contact pressure on wear also in terms of reduction in thickness for the two sets of brake pads at constant rotational speed of 980rpm. From the table, it can be deduced that the average wear rate of pad A at 980rpm is 6.9×10^{-3} mm per brake application while that of pad B is 8.05×10^{-3} mm per brake application. These values are also slightly higher than that of a typical automotive brake pad i.e. 5×10^{-4} mm per brake application (Blau, 2001). Tables 3 show the average stopping time of both sets of brake pads under conditions of varying speed and contact pressure respectively. From the tables, it is evident that pad A has a shorter stopping time than pad B. A micrometer screw gauge was used to measure the reduction in thickness after 30 brake applications. The choice of 30 brake applications was such that an appreciable and measurable reduction in thickness could be obtained after which the average of the values were taken to reflect the reduction in thickness per brake application.

TABLE 1: EFFECT OF SPEED ON BRAKE PAD WEAR AT CONSTANT CONTACT PRESSURE OF 10BAR.

A – REDUCTION IN THICKNESS AFTER 30 BRAKE APPLICATIONS (MM)			B – WEAR PER BRAKE APPLICATION (X10 ⁻³ MM)		
Speed of brake disc(rpm)	Pad A	Pad B	Speed of brake disc (rpm)	Pad A	Pad B
695	0.137	0.172	695	4.56	5.72
884	0.172	0.200	884	5.74	6.68
980	0.190	0.219	980	6.32	7.30
1248	0.235	0.274	1248	7.84	9.12

TABLE 2: EFFECT OF CONTACT PRESSURE ON BRAKE PAD WEAR AT CONSTANT SPEED OF 980 RPM.

A – REDUCTION IN THICKNESS AFTER 30 BRAKE APPLICATIONS (MM)			B – WEAR PER BRAKE APPLICATION (X10 ⁻³ MM)		
Contact pressure (bar)	Pad A	Pad B	Contact pressure (bar)	Pad A	Pad B
8	0.160	0.176	8	5.34	5.87
10	0.190	0.219	10	6.32	7.30
12	0.224	0.264	12	7.45	8.81
14	0.255	0.306	14	8.49	10.21

The above results show that judging by the quality indices selected i.e. wear rate and average stopping time, pad A is of a greater quality than pad B. Furthermore, the wear results show that some of the brake pads currently obtainable in the Nigerian market compare well with international standards. As a precautionary measure, it was ensured that the disc was centrally positioned between the brake pads and also the caliper was carefully selected before purchase to ensure that the automatic adjustment mechanism was functioning properly and its pistons return to their original position once the foot is removed from the brake pedal. These if not done could lead to non uniform wear of a pair of brake pads.

TABLE 3: AVERAGE STOPPING TIME OF BOTH SETS OF BRAKE PADS AT CONSTANT CONTACT PRESSURE OF 10BAR AND CONSTANT SPEED OF 980 RPM.

A – AVERAGE STOPPING TIME (SEC) AT CONSTANT PRESSURE OF 10BAR			B – AVERAGE STOPPING TIME (SEC) AT CONSTANT SPEED OF 980RPM		
Speed of brake disc (rpm)	Pad A	Pad B	Contact Pressure (bar)	Pad A	Pad B
695	3.57	3.74	8	7.34	7.54
884	3.98	4.02	10	6.82	7.01
980	4.13	4.55	12	5.33	6.47
1248	4.67	5.21	14	4.15	5.14

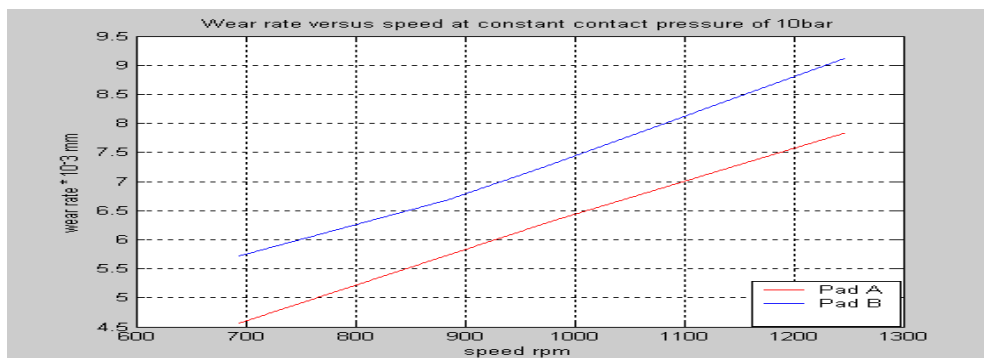


FIGURE 3: WEAR RATE OF TWO BRAKE PAD SAMPLES A AND B PER BRAKE APPLICATION AT A CONSTANT PRESSURE OF 10BAR.

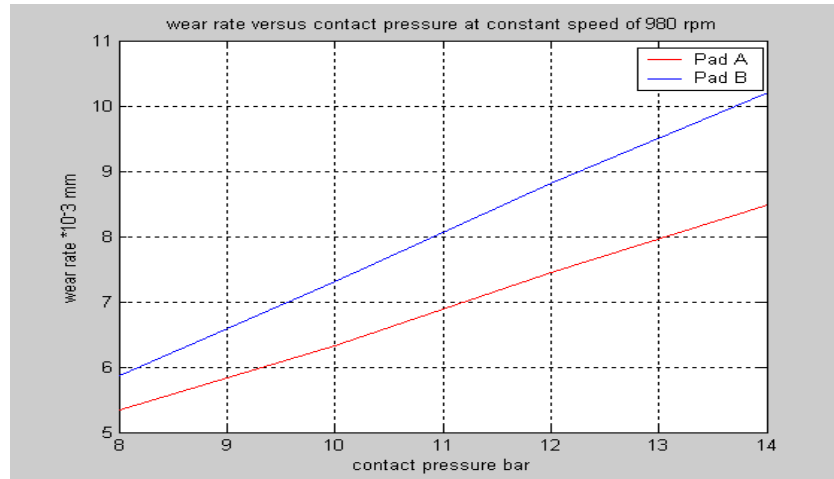


FIGURE 4: WEAR RATE OF TWO BRAKE PAD SAMPLES A AND B PER BRAKE APPLICATION AT A CONSTANT SPEED OF 980RPM.

V. CONCLUSION

The design and construction of the Experimental Brake Pad Test Rig was a successful one. The performance was satisfactory when it was used to determine the wear rate of brake pads. The results obtained were comparable with standard values. This type of equipment is therefore recommended for use in our local automotive friction material manufacturing industries.

VI. ACKNOWLEDGEMENT

The authors are grateful to the supervisor of this work, Engr. J. O. Igbokwe of the department of Mechanical Engineering, Federal University of Technology Owerri, and to our colleague Nwachukwu Anthony Nnadozie for their contribution towards the success of this work.

REFERENCES

- [1] **Baker, A.K. (1992):** Industrial Brake and Clutch Design, Pentech Press Limited; London.
- [2] **Blau, P.J. (2001):** Compositions, Functions and Testing of Friction Brake Materials and Their Additives. A Report by Oak Ridge National Laboratory for U.S. Department of Energy.
- [3] **Borjesson, M. (1993):** "The Role of Friction Films in Automotive Brakes Subjected to Low Contact Forces". Proceedings of the Institution of Mechanical Engineers, Part C.
- [4] **Bush, H.D. Rowson, D.M. and Warren, S.E. (1972):** "The Application of Neutron Activation Analysis to the Measurement of Wear of A Friction Material", Wear.
- [5] **Dagwa I. M and Ibadode A. O. A. (2005):** "Design and Manufacture of Experimental Brake Pad Test Rig"; Nigerian Journal of Engineering Research and Development (NJERD) Vol. 4, No. 3, Ondo, Nigeria. Pp. 15-24.
- [6] **Deutschman, A.D. Michels, W.J. and Wilson, C.E. (1975):** Machine Design Theory and Practice; Macmillan Publishing Co; Inc. New York.
- [7] **Eriksson, M. and Jacobson, S. (2000):** "Tribological Surfaces Of Organic Brake Pads", Tribol Intern.
- [8] **Giri, N.K. (2005):** Automobile Technology; Khanna Publishers; Nai Sarak, Delhi.
- [9] **Halling, J. (ed) (1987):** Principles of Tribology; Macmillan Education Publishers, London.
- [10] **Hutchings, I.M. (1992):** Tribology: Friction and Wear of Engineering Materials; Edward Arnold Publishers; London.
- [11] **Kao, T.K. and Richmond, J.W. (1993):** "Computational Analysis of Disc Pad Performance." Proceedings of the Institute Of Mechanical Engineers.
- [12] **Khurmi, R.S. and Gupta, J.K. (2005):** Machine Design, Eurasia Publishing House, New Delhi.
- [13] **Mudd, S.C. (1986):** Technology for Motor Mechanics, Second Edition; Pruitmarks, Ibadan.
- [14] **Oguzie, G.C.N. (2001):** Vehicle Technology and Workshop Practice; Ihem Davis Press Limited, Owerri.
- [15] **Onwuka, D.O. (2001):** Strength of Engineering Materials, Unique Books, Nigeria.
- [16] **Read, P.P.J. and Reid, V.J. (2000):** Motor Vehicle Technology For Mechanics, Macmillan Education Publisher; London And Busingstoke.
- [17] **Rhee, S.K. (1974):** "Wear Mechanism For Asbestos-Reinforced Automotive Friction Materials", Wear.
- [18] **Smales, H. (1995):** "Friction Materials- Black Arts or Science?" Proceedings of the Institution of Mechanical Engineers, Part D.
- [19] **Shigley, J.E., Mischke, C.R. and Budynas, R.G. (2004):** Mechanical Engineering Design, 7th Ed., McGraw Hill, New York.
- [20] **Stefanovic, I. (2004):** "Tribo-Mutations in Automobile Brake Pads", World Congress of Automotive Engineers; Barcelona, Spain.
- [21] **Weintraub, M. (1998):** Brake Additives Consultant. Private Communication.